Scintigraphic Monitoring of Mucociliary Tracheo-Bronchial Clearance of Technetium-99m Macroaggregated Albumin Aerosol

S. Tzila Zwas, Ido Katz, Benjamin Belfer, Gerald L. Baum, and Ephraim Aharonson

Department of Nuclear Medicine and the Pulmonary Division, Department of Medicine, The Chaim Sheba Medical Center, Tel-Hashomer the Sackler School of Medicine, Tel-Aviv University, and the Biological Institute, Ness-Ziona, Israel

A simple method for in vivo monitoring mucociliary tracheo-bronchial clearance is described. Eighteen healthy subjects and 13 patients with various chronic lung diseases were studied by this method. The principle of using an aerosol administration system similar to the system used for routine ventilation lung studies is stressed. Proximal large airway deposition of the radioaerosol was obtained by using relatively large particles (average diameter 2 μM) of [^{99m}Tc]MAA aerosol. Monitoring was performed by visual inspection of the tracheo-bronchial cinescintigraphic ascendence of the accumulated radioactive boli and by assessing their rate of clearance via automated computer analysis of the time-activity curves, following the movement of each bolus. The normal mean ± s.d. clearance rate thus obtained was 4.7 ± 1.3 mm/min. This rate appears to be more precise as compared with the range of results obtained by other radioisotopic methods. Significantly faster rates, mean 8.2 ± 1.4 mm/min ($p < 0.001$) were obtained in bronchiectatic patients while slower rates (2.8 mm/min) were seen in a patient with ciliary dyskinesia.

J Nucl Med 28:161–167, 1987

Disorders of the mucociliary transport system play a major role among nonrespiratory functions in causing congenital (*1*) and acquired (*2–4*) bronchial diseases. Primary (congenital) ciliary dyskinesia (PCD) is eventually associated with bronchiectasis. Early recognition of PCD and aggressive therapy have appeared to change the natural history of the disease (5). The recognition of impairment of mucociliary clearance (MCC) secondary to various diseases (*6,7*) and conditions, and the need to evaluate the effect of drugs (*7*) on MCC, has led to a search for a reliable method to evaluate mucociliary transport and to the development of several relatively complex techniques. These include fiberoptic (*8*), radiologic (*9*), and radioisotopic methods, the latter utilizing complicated closed systems for inhalation of radioisotopic powders or aerosols (*10–18*).

Received Apr. 23, 1985; revision accepted Aug. 8, 1986.

For reprints contact: S. Tzila Zwas, MD, Dept. of Nuclear Medicine, The Chaim Sheba Medical Center, Tel-Hashomer 52621, Israel.

In the present paper a simple, noninvasive, and reliable in vivo method of monitoring the tracheo-bronchial mucociliary transport rate is reported.

MATERIALS AND METHODS

Healthy Subjects

Eighteen subjects, seven females and 11 males (mean age 33 yr; range 19–60 yr) gave informed consent and were entered into the study which had been approved by Chaim Sheba Medical Center Committee on Human Experimentation. All were healthy, nonsmoking individuals without any pulmonary abnormality as verified by a standard respiratory questionnaire and pulmonary function studies.

Patients

The method was applied to 13 patients with chronic lung diseases, six females and seven males, age range 19–75 yr, average 44 yr; three patients with chronic obstructive airway disease, one patient with sarcoidosis, stage III, eight patients with bronchiectasis and normal cilia, and one patient with bronchiectasis and the primary ciliary dyskinesia syndrome.

Radioaerosol Preparation and Administration

Technetium-99m macroaggregated albumin ([^{99m}Tc]MAA) was prepared using a kit supplied by the Nuclear Research Center, Israel Atomic Energy Commission. Three to four milliliters of [^{99m}Tc]sodium pertechnetate solution containing 15–20 mCi/ml were added to the dry powder and the suspension was incubated at room temperature for 15 min. The ^{99m}Tc-labeled MAA suspension was transferred to a positive pressure nebulizer attached to a disposable radioaerosol administration system* designed by Taplin et al. (*19*) for radioaerosol ventilation lung studies.

The positive pressure nebulizer was connected to an oxygen outlet and attached to disposable tubing leading to a settling reservoir. Additional tubing connected the bag to a mouthpiece through a two-way breathing valve. The tubing leaving the mouthpiece was connected to a bacteria filter which trapped any aerosol obtainable from the patients' exhaled air (diagram in Ref. *19*).

After explaining the procedure to the subject and filling the nebulizer with the [^{99m}Tc]MAA solution, the oxygen flow was turned on at a rate of 6–8 l/min and the bag was filled with aerosol. At this point the subject was instructed to breathe through the mouthpiece in a sitting position and simultaneously a nose clip was attached to him and the bag outlet tubing was unclamped. Normal (tidal breathing) was maintained and the tagged material inhaled with typical count rate over the posterior chest of 2,000 cps indicating that 0.5–0.6 mCi were retained. The inhalation period required to obtain this count rate was usually 3 min (range 2–4 min). The oxygen flow was turned off whenever the bag was full and back on when the bag appeared half full. This had to be repeated several times during the inhalation procedure. Upon completion of the inhalation, the subject rinsed his mouth thoroughly to remove radioaerosol from the oral cavity.

Aerosol Size Characterization

The nebulized [^{99m}Tc]MAA particles used for inhalation were sampled at the mouthpiece of the aerosol administration system by a calibrated eight-stage cascade impactor.† The impactor was operated at a constant flow-rate of 8 l/min and the amount of radioactivity tagged aerosol trapped by each stage was measured in a gamma well counter.‡ The size distribution obtained fitted a log-normal curve with a mass median aerodynamic diameter of the [^{99m}Tc]MAA particles of 2.0 μM and a geometric standard deviation of 2.0.

Image Acquisition and Processing

In preliminary studies we observed that boli started traveling up the trachea after 10–40 min. This phenomenon was also observed by others (*15*). Because of that, a 30-min interval postinhalation in a sitting position was used to allow the perihilar and peripherally deposited particles to accumulate in the hilar and tracheo-bronchial regions. Then, the subject was placed supine beneath the gamma camera which was interfaced with a computer. The field-of-view included the neck and both lungs in anterior view centered on the tracheobronchial regions. The subject remained immobile during a 40-min acquisition period. The data were acquired in the form of 30-sec 64 × 64 byte-mode frames and stored in the computer for further analysis. Two cobalt-57 point sources affixed exactly 10 cm apart on a rigid scale were placed within the camera field-of-view, but clear of the lungs for the duration of the first 30-ft frame, enabling subsequent scaling of the image in mm/pixel. In order to prevent inaccuracies arising due to possible changes in the spatial calibration, this procedure was repeated for each study.

Discrete radiomucous boli were formed in the tracheobronchial area and could be seen to ascend the trachea as time progressed. A program module was prepared to calculate the ascendence speed of these boli in mm/min:

The computer-stored images were first viewed to select boli suitable for calculating the rate of ascendence. Suitable boli showed a distinctive and well demarcated focus of radioactivity which could be observed to consistently ascend along the tracheal canal (Fig. 1A).

These frames were summed so as to pursue optimal visualization of the tracheo-bronchial regions, and up to 16 regions of interest (ROIs) were drawn contiguously along the length of trachea, each ROI being of a standard height of 2 pixels (Fig. 1B).

The number of pixels separating the point sources incorporated in the first frame (10 cm apart) was counted, and the image scale in pixels was calculated. The uncertainty in this procedure was estimated to be ±1 pixel resulting in an uncertainty of ±5% in the spatial scaling.

Time-activity curves (TACs) were then generated for each of the ROIs over the 80 frames (Fig. 1C). The passage of a radiomucus bolus through a given ROI was indicated by a characteristic peak appearing in the corresponding TAC, and the coherent advance of this bolus along the trachea was recognized by the advance of this peak along the time axis in the TACs from ROI to ROI (Fig. 1C).

Thus in advancing from one point to another along the trachea, spatial position was given by the ROI number and the time elapsed was noted on the TAC abscissa in units of frame numbers: 1–80.

The mean speed of advance (S) of each mucous bolus was given by the formula:

$$S_{(mm/min)} = \frac{H_R \times C \times (R_F - R_I)}{T_F \times (F_F - F_I)}, \qquad (1)$$

where H_R = height of ROI in pixels (constant), C = image scale in mm/pixel (constant) R_F, and R_I are the final and initial ROIs used for the calculation (Fig. 1C). The monitored bolus peak is indicated by the arrows. F_F and F_I are the corresponding frame numbers for the bolus peak, and T_F = frame time in minutes (constant). After inspection of the TACs for a suitable bolus indicated by a peak seen in several frames and showing maximal radioactivity advancing linearly through contiguous ROIs, the data were fed into the computer, and the mean rate of advance was calculated by formula (1) and printed out together with all the TACs (Fig. 1C, D).

Lung Dosimetry Measurements

The initial postinhalation image served to measure radioactive aerosol deposition over three areas of interest, namely the lung fields, trachea, and the pharynx. From a previous calibration of the camera's sensitivity (3,500 cps/mCi), the retention of aerosol particles in the three areas could be measured, since the count rate over any ROI never exceeded the camera's maximal count rate capabilities without data loss (which is 60,000 cps). The retentions found were respectively, 600 μCi (2,100 cps), 60 μCi (200 cps), and 10 μCi (30 cps),

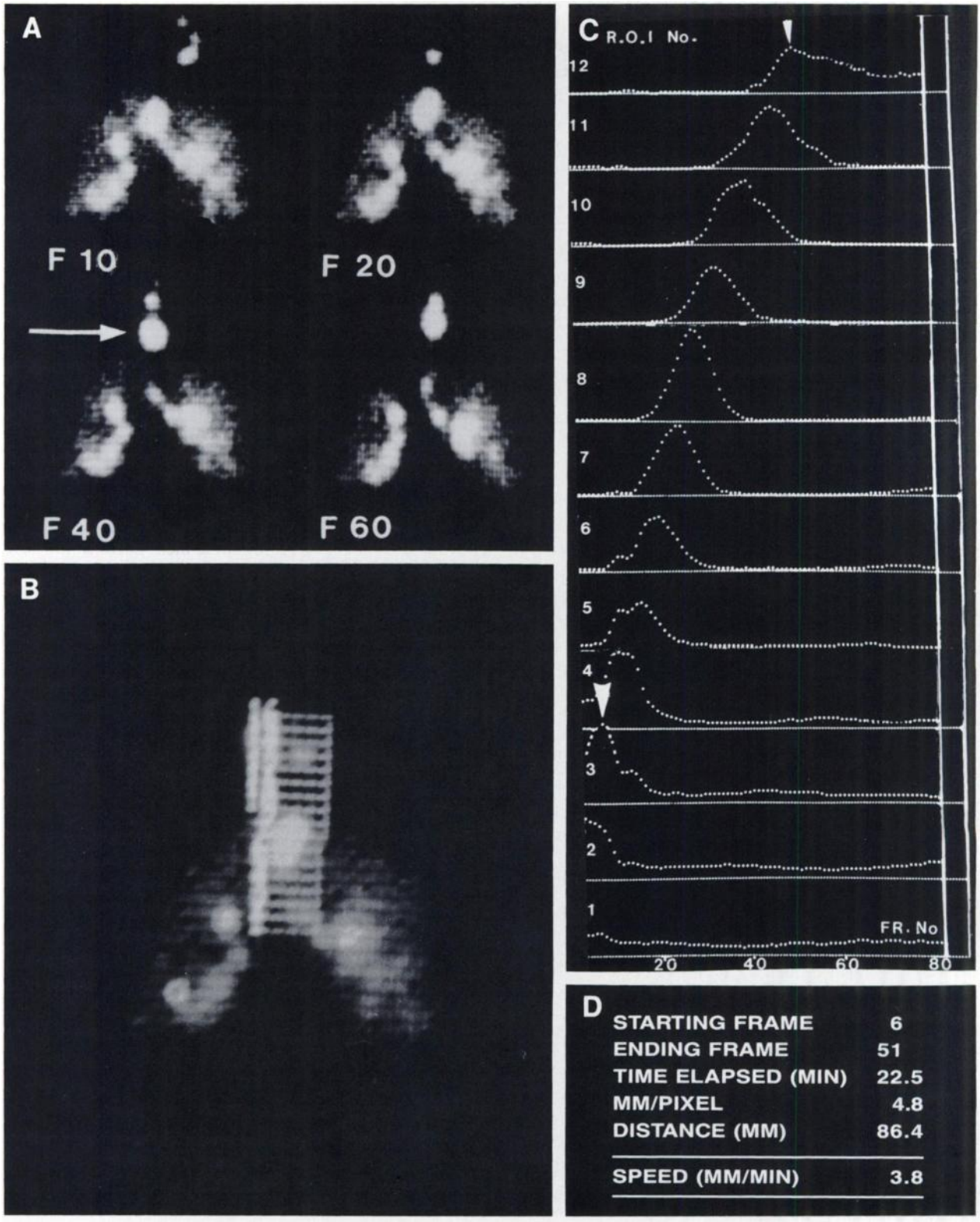

FIGURE 1

Case 15, (see Table 1). Typical mucociliary clearance study demonstrating stages of monitoring [^{99m}Tc]MAA-labeled mucous boli in the tracheo-bronchial region (sections A–D). A: Four sequential anterior chest images in time intervals indicated by F (frame) numbers (30 sec/F): A radiolabeled bolus is seen (arrow) to ascend the tracheal channel. B: Computer summation of frames 1–80 with superimposed contiguous ROIs outlining the tracheal channel. C: Computer display of the time-activity curves (TACs) corresponding to the ROIs in section (B). The peak of radioactivity represents the radiolabeled bolus shown in section (A). Bolus peak is indicated in the initial and final TACs: 3 and 12, respectively (arrowheads). Continuous linear advance of the bolus peak is demonstrated throughout the consecutive TACs. D: Final data calculated from the TACs in (C). The clearance rate of the radiolabeled mucous bolus was calculated using formula (1)—see text.

for the lung fields, oropharyngeal region, and the tracheal regions. These are estimated to deliver 0.3 rad (*20,21*), 30 mrad, and 5 mrad, respectively.

RESULTS

The deposition patterns of the [^{99m}Tc]MAA particles in the normal subjects are shown in the scintigrams illustrated in Figure 1A. Some of the aerosol was deposited in the throat or larynx probably due to turbulence and impaction. High concentrations of activity were located centrally in the lungs, while very little activity was located in the lung periphery.

Radioactive boli were seen to move up to the main bronchi after alternately accumulating in both hili and ascending towards the carina. From the carina each bolus either joined other concentrations or continued its ascent upwards towards the pharyngeal region. Several boli were seen in each study successively ascending the trachea in a constant movement. Visually, none of the scintigrams demonstrated retrograde or spiral movement, but a temporary standstill of a few boli was noted at the carina region. The left hilar region demonstrated a faster clearance compared to the right in two-thirds of the normal studies. Two suitable radiomucous boli were monitored during each of the studies and the resulting rates of each of the two boli were recorded.

The personal data of the subjects and the mucociliary clearance rates of each radioactive bolus measured in the 18 normal studies are summarized in Table 1. The mean mucociliary clearance rate of the total of 36 boli was 4.7 ± 1.3 mm/min (X ± s.d.), (CV% = 27) with a range of 2.6–6.4 mm/min. The intersubject differences in the dual boli measurements were 26% mean; 2–78% range. No significant differences in MCC rates could be found between males and females or in different ages among the normal subjects in this study.

TABLE 1
Personal Data and Radioaerosol Tracheo-Bronchial Mucociliary Clearance Results in 18 Healthy Subjects

Subject no.	Age(yr)/ sex	Mucociliary clearance rates (mm/min) First bolus	Second bolus	Mean
1	33 M	7.9	4.9	6.4
2	32 M	3.1	2.8	3.0
3	27 M	7.8	5.4	6.6
4	35 F	4.5	8.0	6.3
5	27 M	2.8	2.3	2.6
6	19 F	4.3	4.7	4.5
7	30 F	5.5	5.0	5.3
8	31 M	2.7	3.0	2.9
9	35 F	5.0	4.9	5.0
10	19 F	3.7	2.7	3.2
11	25 F	6.4	5.4	5.9
12	26 M	4.2	4.8	4.5
13	25 M	3.7	3.6	3.7
14	25 M	3.4	4.4	3.9
15	22 F	3.8	3.6	3.7
16	60 M	5.7	6.1	5.9
17	60 M	5.5	4.8	5.2
18	59 M	5.3	6.6	5.8
	Mean ± s.d.	4.7 ± 1.5	4.6 ± 1.4	4.7 ± 1.3
	CV%	31.9	30.4	27.2

The personal, clinical, and respiratory function studies in the 13 patients group are given in Table 2. All patients were clinically stable at the time of the study and had refrained from using any medication for at least 4 hr, prior to the study. Each patient underwent MCC study where dual boli measurements were obtained resulting in a total of 26 measurements. The studies were performed in a supine position as with the normal controls. These scintigraphic data are given in Table 3.

The deposition patterns of the radioaerosol particles demonstrated in general a centrally located distribution with major retention in the proximal airways, particularly in the bronchiectatic group, and somewhat less in patients with COPD. Increased rates of MCC were measured in patients with bronchiectasis with typically large amounts of small irregular boli accumulating fast and disappearing up in the trachea. In studies of a few bronchiectatics and severe COPD cases, remarkably large boli were observed accumulating in excessive amounts with a fast clearance rate. MCC measurements showed (Table 3) significantly higher than normal rates in the bronchiectatic group (mean 8.2 ± 1.5, (CV% = 17) range 7.2–10.7 mm/min) and rates in the upper limit of the normal range in the COPD group (mean 5.7 ± 0.4, (CV% = 7) range 5.2–6.3 mm/min). In the one patient with primary ciliary dyskinesia (No. 13) the initial pattern of particle deposition was similar to the typical bronchoectatic group, but the boli appeared in the tracheobronchial region after a significant delay and were scanty, small and had irregular clearance motion. The MCC rate was slow, in the lower limit of the normal range. The intra-patient differences in the dual boli measurements were 9% mean; 0–24%, range. Thus, the overall reproducibility and precision of MCC rate measurements in the patients was higher than in the control group (Table 1), with lower intra- and interpatient variation (Table 3), indicating a more homogeneous distribution of the MCC rates within patients with similar pulmonary pathology.

The examination caused no untoward effects or discomfort to the patients and was simple to perform in all our studies.

DISCUSSION

A ciliated epithelium lines the respiratory channels from the nose to the terminal bronchioles. This ciliated

TABLE 2
Patients Clinical Diagnoses and Pulmonary Function Status

Case no.	Diagnosis	FVC* (l)	(% Pred.)	FEV_1† (l)	(% Pred.)	$\dot{V}_{50}$‡ (l/sec)	Misc.
1	COPD	2.4	(44)	1.3	(28)	0.6	RV§ = 222% PO¶ = 65 PCO_2** = 40.6
2	COPD Asthma	3.3	(76)	2.7	(73)	3.1	
3	COPD	1.8	(44)	0.7	(20)	0.3	
4	Sarcoidosis stage III	2.9	(68)	1.8	(53)	1.4	PO_2 = 79 PCO_2 = 36
5	Cystic fibrosis bronchiectasis	2.9	(66)	1.6	(42)	1.1	RV = 141% PO_2 = 79.4 PCO_2 = 39
6	Bronchiectasis	4.4	(77)	3.8	(77)	7.2	RV = 89% PO_2 = 100 PCO_2 = 40
7	Bronchiectasis	2.2	(49)	1.6	(44)	1.5	RV = 220% PO_2 = 90 PCO_2 = 35
8	Severe bronchiectasis	1.7	(43)	0.6	(21)		PO_2 = 65.3 PCO_2 = 36.5
9	Bronchiectasis	2.7	(70)	1.8	(63)	1.3	RV = 117%
10	Severe bronchiectasis	1.3	(40)	0.8	(33)	0.7	RV = 109%
11	Severe bronchiectasis	2.5	(77)	1.7	(67)	1.9	RV = 149%
12	Bronchiectasis	1.3	(45)	0.6	(24)	0.3	
13	Ciliary dyskinesia (Kartagener's Syndrome)	4.8	(87)	2.8	(64)		RV = 194%

* FVC = Forced vital capacity.
† FEV_1 = Forced expiratory volume in one second.
‡ $\dot{V}_{50}$ = Maximum expiratory flow at 50% vital capacity.
§ RV = Residual volume.
¶ PO_2 = Oxygen partial pressure in arterial blood-Torr.
** PCO_2 = Carbon dioxide partial pressure in arterial blood-Torr.

epithelium is covered by a two-phase fluid: a periciliary serous layer and a supraciliary mucous layer which is continuously being cleared from the periphery of the lung towards the tracheo-pharyngeal exit, from where it is eliminated by swallowing. This constant mucociliary clearance serves as an effective cleansing mechanism for the tracheo-bronchial tree.

The integrity of this clearance system guarding against retention of foreign particles within the lungs is of great importance. Thus objective assay of the system is essential to recognizing and understanding abnormalities. Efficient in vitro assay for evaluation of ciliary-beat-frequency (CBF) exists (*22,23*). In vivo monitoring of mucociliary clearance however, has the major advantage of including all components affecting the clearance function as a whole, e.g., mucous composition, size and configuration of the airways, neurogenic influences, etc, as well as ciliary activity.

Two main mechanisms of lung clearance have been investigated: the peripheral (alveolar) lung clearance (*10,15,16,18*) and tracheo-bronchial-extrapulmonary clearance measurements (*11–18*). In other words, ideally the nonciliated lung and ciliated tracheo-bronchial clearance can be measured separately. It is clear, however, that peripheral clearance does indeed involve terminal ciliated mucosa, and the central clearing mechanism is functionally related to the nonciliated tracheo-bronchial tree. The technique herein reported deals with evaluation of central clearance and its relationship to ciliated mucosae. Previous studies using various radiological and radioisotopic methods showed a marked difference in the rate of clearance between lung periphery and central zones of the tracheo-bronchial tree (*15, 17,18*) with an increasing rate of clearance as the channels enlarge; therefore, it is slowest in the lung periphery.

Various methods have been used to monitor different zones of the lungs and/or central airways with variable success, due mainly to the complexity of the methods employed. Each study reported on different parameters, and results have not been comparable or reproducible (*10–18*). In contrast, results with the radioisotopic monitoring system described in this report suggest the following conclusions.

1. It is possible to use a simple disposable aerosol administration system available commercially and well

TABLE 3
Patients Personal Data and Radioaerosol Mucociliary Clearance Results

Case no.	Age(yr)/ sex	First bolus	Second bolus	Mean
COPD				
1	24 M	5.0	5.7	5.4
2	43 M	4.6	5.7	5.2
3	61 M	5.5	6.6	6.0
4*	50 M	6.0	6.6	6.3
	Mean	5.3 ± 0.5	6.2 ± 0.45	5.7 ± 0.4
	CV%	9.4	7.2	7.0
Bronchiectasis				
5	25 F	8.0	8.5	8.3
6	19 M	8.5	8.5	8.5
7	29 F	6.6	8.0	7.3
8	47 F	7.7	6.6	7.2
9	75 M	10.0	11.4	10.7
10	62 F	10.5	9.3	9.9
11	52 F	6.0	6.6	6.3
12	61 F	8.0	7.0	7.5
	Mean	8.2 ± 1.4	8.2 ± 1.5	8.2 ± 1.4
	CV%	17.0	18.3	17.0
Mucociliary dyskinesia				
13	29 M	2.7	2.9	2.8

*Stage III sarcoidosis with airways obstruction.

TABLE 4
Tracheo-Bronchial Mucociliary Clearance Results (in Healthy Subjects)

Authors	No. of cases	Clearance rates (mm/min) Mean + range
Yeates DB (9) 1975	42	4.7 (0.8–12.8)
Ross TH (11) 1979	7	9.0 (2.0–17.0)
Yeates DB (12) 1981	22	5.1 (2.2–8.0) ± 2.9 (s.d.)
Current study	18	4.7 (2.6–6.4) ± 1.3 (s.d.)

established for use in ventilatory lung studies. Thus the same system can be used for both ventilation and mucociliary clearance assays. Other inhalation systems with appropriate means for particle size and air flow rates adjustments can be used for this purpose.

2. Relatively large size particles result in proximal aerosol deposition in the central tracheo-bronchial zones forming localized boli of labeled mucus. This offers a shorter monitoring time due to faster particle transport in the highest motility zone, as opposed to greater clearance variations that occur in the lung periphery (*17,18,24–26*).

3. Monitoring individual boli ascending the tracheal channel is here achieved by direct visual assessment in an analog and computerized cine-mode display. The suggested method of computer analysis has two advantages. (A). It is possible to monitor several boli and to determine the rate of clearance for each of the several visualized boli independently during the examination, thus further increasing the precision of this in vivo procedure. The dual measurements performed in all of our cases lowered the CV% of the mean results by about 4% as compared to single measurements in the control group and 1–2% in patient studies (Tables 1, 3). According to the paired "t" test there was no significant difference when performing single or dual measurements or measuring the first or the second bolus in each study (with $t = 0.65$). Therefore dual measurements of clearly visualized boli in each study seems adequate. (B). Calculation variabilities are eliminated using an automated system with a preset processing protocol and standardized ROI drawing criteria and velocity measurements.

4. It is possible to compare tracheo-bronchial mucosal function with function of the cilia in other organs such as the nose (*22,23*).

The results obtained in our study with normal subjects and in patients with various lung diseases appear more precise than the ranges of velocity obtained by other radioisotopic methods in the tracheo-bronchial region (*11–18*). Table 4 summarizes other normal results from the literature, obtained with various radioisotopic methods using comparable parameters for clearance measurements. Our method has the advantages of simplicity and ease of performance as well as high monitoring precision. The clinical usefulness of this method in patients with lung disease was demonstrated by the MCC results and distinctive scintigraphic (boli) patterns noted in patients with COPD, bronchiectasis and mucociliary dyskinesia. Significantly higher ($p > 0.001$) MCC rates appears in bronchiectatic patients, as compared to patients with COPD and normal subjects, while the one patient with ciliary dyskinesia who presented clinically with bronchiectasis had a MCC rate at the lower limit of normal. Thus, it appears that the method of assay of MCC reported here may provide useful information in evaluation of patients with a variety of bronchial diseases.

NOTES

*(Model No. 177-061) Atomic Products Co., Shirley, NY.
†(Stack sampler mark III) Anderson Inc.
‡Picker International, Highland Heights, OH.

ACKNOWLEDGMENTS

This work was supported by a grant from the Chief Scientist's Office, the Ministry of Health, Israel.

The authors thank Lionel M. Lieberman, MD, PhD, for helpful review of the manuscript.

REFERENCES

1. Eliasson R, Mossberg B, Camner P, et al. The immotile cilia syndrome. A congenital ciliary abnormality

as an etiologic factor in chronic airway infections and male sterility. *N Engl J Med* 1977; 297:1–6.
2. Mossberg B, Afzelius BA, Eliasson R, et al. On the pathogenesis of obstructive lung disease: a study in the immotile-cilia syndrome. *Scan J Respir Dis* 1978; 59:55–65.
3. Kollberg H, Mossberg B, Afzelius BA, et al. Cystic fibrosis compared with the immotile-cilia syndrome. A study of mucociliary clearance, ciliary ultrastructure, clinical picture, and ventilatory function. *Scan J Respir Dis* 1978; 59:297–306.
4. Rossman CM, Forrest JB, Ruffin RE, et al. Immotile cilia syndrome in persons with and without Kartagener's syndrome. *Am Rev Respir Dis* 1980; 121:1011–1016.
5. Yarnal JR, Golish JA, Ahmad M, et al. The immotile cilia syndrome. *Postgrad Med* 1982; 71:195–217.
6. Mygind N, Pedersen M, Nielsen MM. Primary and secondary ciliary dyskinesia. *Acta Otolaryngol* 1983; 95:688–694.
7. Pavia D, Sutton PP, Lopez-Vidriero MT, et al. Drug effects on mucociliary function. *Eur J Respir Dis* 1983; 64:304–317.
8. Sackner MA, Rosen MJ, Wanner A. Estimation of tracheal mucus velocity by bronchofiberoscopy. *J Appl Physiol* 1973:495–499.
9. Clarke SW, Pavia D. Comparison of techniques for measuring tracheal mucous velocities *in-vivo* in man. In: Nakhosteen JA, Maassen W, eds. Bronchology: research, diagnostic, and therapeutic aspects. The Hague/Boston/London: Martinus Nijhoff Publishers, 1981:469–471.
10. Lourenco RV, Klimek M, Borowski CJ. Deposition and clearance of 2 particles in the tracheo-bronchial tree of normal subjects—smokers and non-smokers. *J Cin Invest* 1971; 50:1411–1420.
11. Albert RE, Lippmann M, Peterson HT, et al. Bronchial deposition and clearance of aerosols. *Arch Intern Med* 1973; 131:115–127.
12. Yeates DB, Aspin N, Levison H, et al. Mucociliary tracheal transport rates in man. *J Appl Physiol* 1975; 39:487–495.
13. Chopra SK, Taplin GV, Elan D, et al. Measurement of tracheal mucociliary transport velocity in humans—smokers versus non-smokers. *Am Rev Respir Dis* 119 (suppl):205, 1979.
14. Ross ITH, Wallace JC, Waite D. A simplified method of monitoring muco-ciliary transport. *Br J Radiol* 1979; 52:968–971.
15. Yeates DB, Pitt BR, Spektor DM, et al. Coordination of mucociliary transport in human trachea and intrapulmonary airways. *J Appl Physiol* 1981; 51:1057–1064.
16. Puchelle E, Aug F, Zahn JM, et al. Comparison of nasal and bronchial mucociliary clearance in young non-smokers. *Clin Sci* 1982; 62:13–16.
17. Pavia D, Sutton PP, Agnew JE, et al. Measurement of bronchial mucociliary clearance. *Eur J Respir Dis* 1983; 64(suppl 127):41–56.
18. Agnew JE, Bateman JRM, Pavia D, et al. A model for assessing bronchial mucus transport. *J Nucl Med* 1984; 24:170–178.
19. Taplin GV, Chopra SK. Inhalation lung imaging with radioactive aerosols and gases. *Prog Nucl Med* 1978; 5:119–143.
20. Pircher FJ, Knight CM, Barry WF, et al. Retention, distribution and absorption of inhaled albumin aerosol and absorbed dose estimates from its I-131 and Tc-99m labels. *Am J Roentgenol* 1967; 100:813–821.
21. Prato FS, Vinitski S. Radiation dose calculations for inhalation of Tc-99m sulfur colloid radioaerosol. *J Nucl Med* 1983; 24:816–821.
22. Rutland J, Griffin WM, Cole PT. Human ciliary beat frequency in epithelium from intrathoracic and extrathoracic airways. *Am Rev Respir Dis* 1982; 125:100–105.
23. Baum G, Roth Y, Teichtahl J, et al. Ciliary beat frequency of respiratory mucosal cells: comparison of nasal and tracheal sampling sites. *Am Rev Respir Dis* 1982; 125:244.
24. Wolf RK, Dolovich M, Eng P, et al. Sulfur dioxide and tracheobronchial clearance in man. *Arch Environ Health* 1975; 30:521–527.
25. Isawa T, Teshima T, Hirano T, et al. Mucociliary clearance mechanism in smoking and non-smoking normal subjects. *J Nucl Med* 1984; 25:352–359.
26. Isawa T, Teshima T, Hirano T, et al. Lung clearance mechanisms in obstructive airways disease. *J Nucl Med* 1984; 25:447–454.